

# Semicircular Ridges in Rectangular Waveguides\*

J. VAN BLADEL† AND O. VON ROHR JR.‡

**Summary**—The two-dimensional Helmholtz equation is solved in a rectangle having two semicircular projections in the center of its broad faces. More particularly, the lowest two eigenvalues are determined for Neumann's boundary condition, and the lowest eigenvalue for Dirichlet's boundary condition. The results are of interest in various fields of physics, such as vibrations of a membrane, but are of particular importance in the study of waveguide propagation. The latter application is stressed in the article, in accordance with the practical importance of ridged waveguides.

## INTRODUCTION

THE LOWEST mode of a rectangular waveguide, *i.e.*, the  $TE_{10}$  mode, has a cutoff frequency  $f_1$  equal to  $c/2a$ , where  $c$  is the velocity of light in the dielectric filling the guide (see Fig. 1). The next to lowest mode is either the  $TE_{01}$  mode, with cutoff frequency  $c/2b$ , or the  $TE_{20}$ , with cutoff frequency  $c/a$ , the choice between these two modes being determined by the aspect ratio  $b/a$  of the cross section. At most, the ratio of the lowest two cutoff frequencies (termed mode separation factor) is seen to be equal to two. Insertion of rectangular ridges has the following effects:<sup>1,2</sup>

- 1) A decrease in the lowest cutoff frequency. This is shown in Fig. 3, where, as in the rest of the article, frequencies are measured in terms of  $c/2a$ . The penetration of the ridge is expressed by the insertion coefficient  $i$ , a quantity which is defined as  $2d/b$  for the rectangular shape and  $2R/b$  for the semicircular shape. In particular,  $i$  takes the value one when the ridges touch each other. It is seen that the presence of the ridges makes the waveguide more compact for any given value of the lowest cutoff frequency.
- 2) An increase in mode separation, as seen in Fig. 6. Consequently, "one-mode" propagation is possible over a broader band of frequencies. This important property has led to the use of ridged waveguide in airborne weather-radar, where the two wavelengths of importance for precipitation detection, *viz.*, 3.2 cm and 5.6 cm, must be alternatively accommodated by the same waveguide run, excite a single mode, and still lie sufficiently far from cutoff values.
- 3) An increase in power attenuation, as evidenced by the two isolated points in Fig. 7. This is objectionable for energy transmission purposes, although

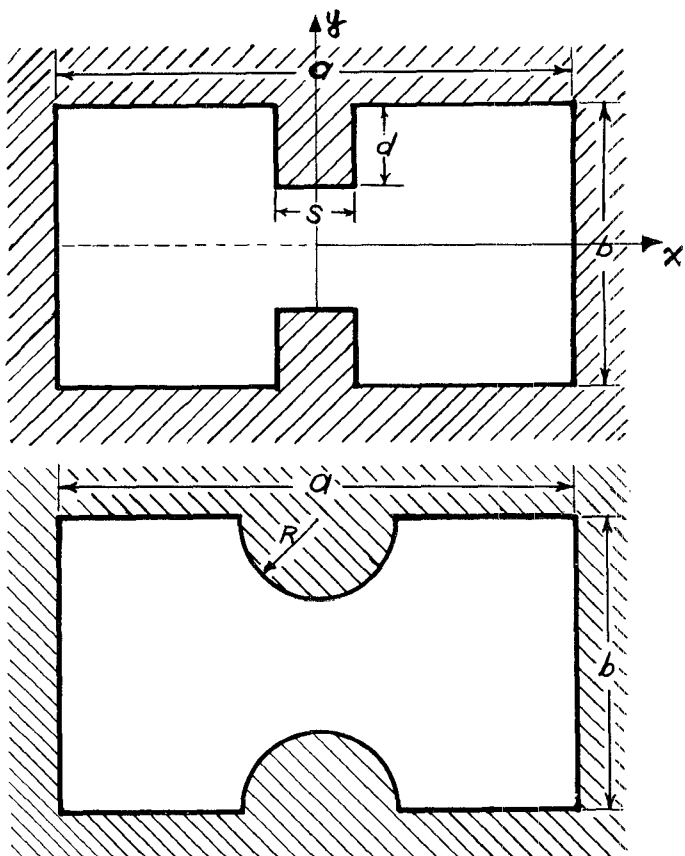


Fig. 1—Rectangular and semicircular ridges.

desirable in the design of certain microwave devices.<sup>1</sup>

- 4) An increase of the maximum electric field intensity in the cross section, namely at the protruding corners of the ridges. This lowers the maximum power which can be transmitted without breakdown. To counteract this effect, corners of the ridge are slightly rounded off in practice. The question then naturally arises as to what would be the effect of rounding off much more drastically, *i.e.*, what desirable and undesirable properties of the rectangular ridge would result when one goes over to the "cornerless" semicircular ridge. It is the purpose of the present paper to give an answer to that question.

## NUMERICAL CALCULATIONS

The structure and properties of a waveguide mode are determined by solving the following two-dimensional eigenvalue problems:<sup>3</sup>

<sup>1</sup> S. B. Cohn, "Properties of ridge wave guide," PROC. IRE, vol. 35, pp. 783-788; August, 1947.

\* Manuscript received by the PGMTT, June 25, 1956.  
† Dept. of Elec. Eng. Univ. of Wisconsin, Madison, Wis. This work was written while the author was at Washington Univ., St. Louis, Mo.

‡ Dept. of Elec. Eng., Washington Univ., St. Louis, Mo.

<sup>2</sup> S. Hopfer, "The design of ridged waveguides," IRE TRANS., vol. MTT-3, pp. 20-29; October, 1955.

<sup>3</sup> S. Ramo and J. R. Whinnery, "Fields and Waves in Modern Radio," John Wiley & Sons, Inc., New York, N.Y., 2nd ed., ch. 8; 1953.

TE modes:  $\nabla^2\phi + k^2\phi = 0$  with

$$\frac{\partial\phi}{\partial n} = 0 \text{ on cross section contour} \quad (1)$$

TM modes:  $\nabla^2\phi + k^2\phi = 0$  with

$$\phi = 0 \text{ on cross section contour.} \quad (2)$$

To each eigenvalue  $k^2$  and eigenfunction  $\phi$  corresponds a different mode, the cutoff frequency of which is equal to  $ck/2\pi$ . The eigenvalue problem of the present article has been solved by classical difference equation methods.<sup>4</sup> Iteration methods have been found more suitable than relaxation methods for the purpose. In brief, the technique consists of starting with a small ridge radius, a coarse net, and a distribution  $\phi^0$  of net point values corresponding to the unperturbed eigenfunction (i.e., relative to the rectangular boundary of same aspect ratio, but without ridge). A first estimate of  $k^2$  is obtained by the Rayleigh quotient

$$(k^0)^2 = \frac{-\sum \phi^0 \nabla^2 \phi^0}{\sum (\phi^0)^2}. \quad (3)$$

Better values of  $\phi$  are obtained by going around the net and replacing the initial values  $\phi^0$  by (see Fig. 2).

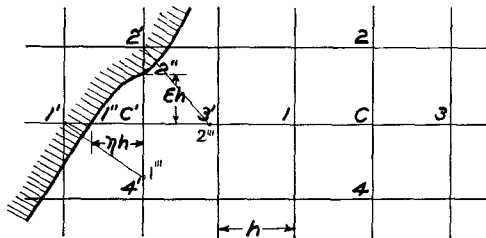


Fig. 2—Points of the nets used in the iteration method.

$$\phi_c' = \frac{\phi_1 + \phi_2 + \phi_3 + \phi_4}{4 - h^2(k^0)^2} \quad (4)$$

for an ordinary point.

$$\phi_c' = \frac{\frac{2}{\eta(1+\eta)}\phi_{1''} + \frac{2}{\epsilon(1+\epsilon)}\phi_{2''} + \frac{2}{1+\eta}\phi_{3''} + \frac{2}{1+\epsilon}\phi_{4''}}{\frac{2}{\epsilon} + \frac{2}{\eta} - (k^0)^2 h^2} \quad (5)$$

for a boundary point.

From this new set of values,  $k^2$  is again computed from (3), and the process is repeated until  $k^2$  converges. One then goes over the finer nets, and computes the corresponding values of  $k^2$ . The final nets, in the present work, contained some 400 points on the average.<sup>5</sup> A typical sequence of values for  $k^2$  is  $11.1/a^2$ ,  $8.3/a^2$ , and

<sup>4</sup> D. N. deG. Allen, "Relaxation Methods," McGraw-Hill Book Co., Inc., New York, N. Y., 1st ed., ch. 5, 6, and 12, 1954.

<sup>5</sup> For more details, see O. Von Rohr's thesis, submitted to the Sever Inst. of Tech. in partial fulfillment of the requirements for the degree of Master of Science in electrical engineering.

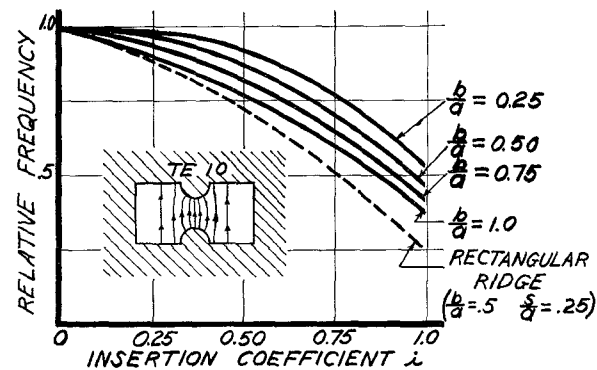


Fig. 3—Cutoff frequency of the lowest mode as a function of the ridge penetration. The dashed curve is relative to a rectangular ridge. The insert shows the lines of force of the electric field in the waveguide cross section.

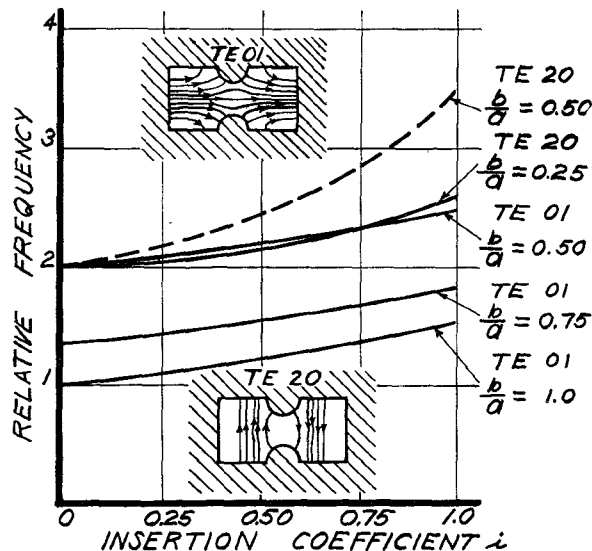


Fig. 4—Cutoff frequency of the second lowest mode as a function of ridge penetration. The inserts show the lines of force of the electric field in the waveguide cross section. The dashed curve, which represents the third lowest mode for  $b/a = 0.50$ , has been added to allow interpolation of the  $TE_{20}$  characteristics between  $b/a = 0.50$  and  $b/a = 0$ .

$7.7/a^2$  for nets containing respectively 19, 97, and 425 points. The extrapolated value, in this particular example, was taken to be  $7.6/a^2$ . The results of the computations are shown in Figs. 3 to 6. Each curve contains five calculated points, and the over-all accuracy is believed to be better than 2 per cent, which is satisfactory for general engineering purposes. Computations were made on a desk calculator, in the absence of a suitable automatic computer. Interest is focused on the lowest two TE modes, which determine the mode separation factor. However, cutoff frequencies of the lowest TM mode have been added, both because it was found desirable to check whether they remain higher than those of the investigated TE modes, and also because they represent the fundamental frequency of the clamped membrane having the contour depicted in the lowest part of Fig. 1. It will be noticed from Fig. 4 that the  $TE_{20}$  mode is the second lowest mode for small aspect ratios. This characteristic property was also displayed by the ridge-

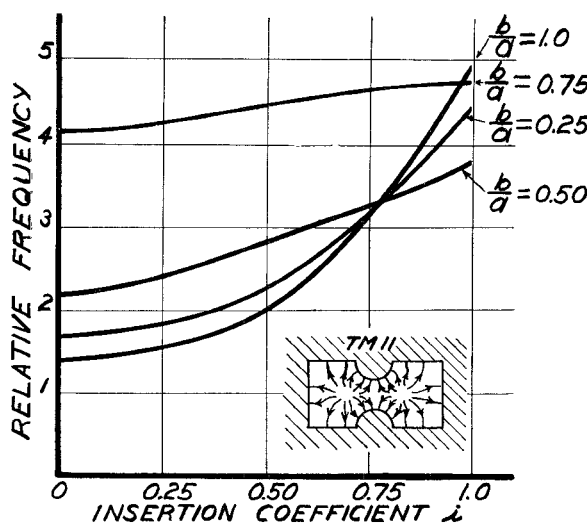


Fig. 5—Cutoff frequency of the lowest TM mode as a function of ridge penetration. The insert shows the lines of force of the electric field in the waveguide cross section.

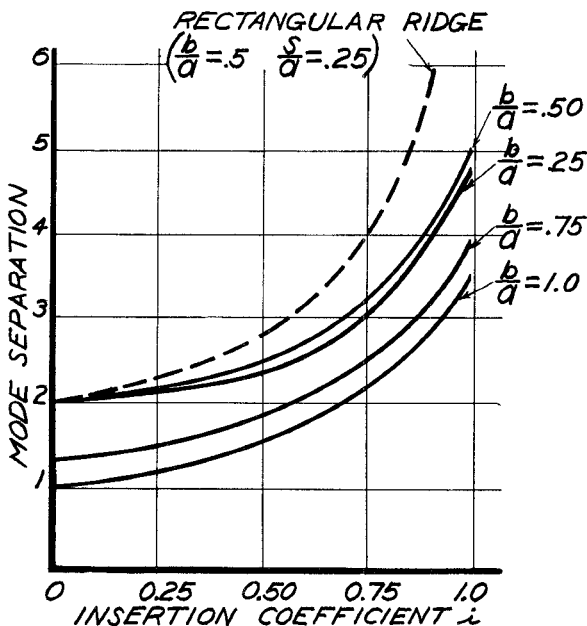


Fig. 6—Mode separation factor as a function of insertion coefficient. The dashed curve, added for comparison purposes, is relative to a rectangular ridge.

less guide. The value of  $b/a$ , however, at which the transition from  $TE_{01}$  to  $TE_{20}$  takes place, is no longer 0.5, but is somewhat smaller. Notice also from Fig. 6 that the mode separation is optimum for an aspect ratio of 0.4 approximately.

The knowledge of the eigenfunction  $\phi$  relative to the lowest mode makes it possible, by using classical formulas,<sup>3</sup> to compute the attenuation and the power handling capacity of the guide. The results are shown in Figs. 7 and 8. It has been found useful, for comparison purposes, to display the attenuation constant relatively to that of a ridgeless rectangular guide of identical material, aspect ratio, and cutoff frequency. The values of the attenuation constant of the latter guide can be found in the literature.<sup>3</sup> The relative power handling

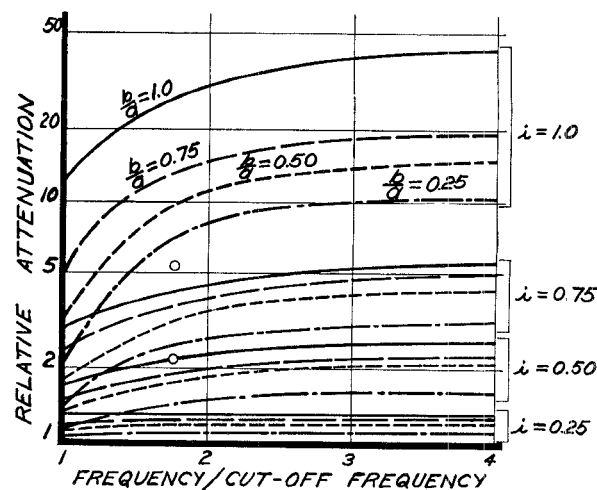


Fig. 7—Attenuation coefficient in terms of the attenuation coefficient relative to a ridgeless waveguide of identical aspect ratio and cut-off frequency. The curves are relative to the lowest mode. The two isolated points refer to the relative attenuation for a rectangular ridge ( $s/a = 0.25$ ,  $b/a = 0.5$ ) of insertion coefficients 0.5 and 0.75 respectively.

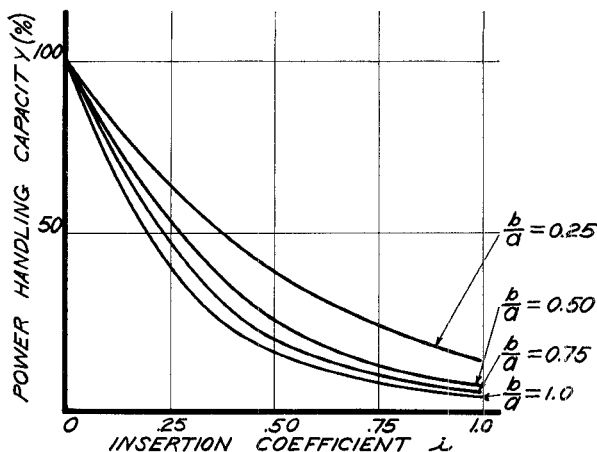


Fig. 8—Decrease of power handling capacity with ridge penetration.

capacity curves indicate that, as the ridge penetration increases, the lowest power level which will cause breakdown (i.e., create, somewhere in the cross section, an electric field equal to the breakdown value) becomes smaller and smaller.

#### Comparison Between Ridges

The best over-all properties, for a rectangular ridge and an aspect ratio of 0.5, are obtained<sup>2</sup> for  $s/a = 0.25$  (Fig. 1). An inspection of Fig. 6 indicates that such a rectangular ridge ensures a better mode separation than the semicircular ridge, for any given insertion coefficient. This is not surprising, for the rectangular ridge covers a larger proportion of the cross section than its semicircular counterpart. The comparison, however, should be made on a mode separation basis. For a given mode separation factor, the semicircular ridge is evidently greatly superior as far as power handling capacity is concerned. The latter is actually zero for a rectangular ridge (that is, if we take maximum local electric field as

a criterion). The relative attenuations are roughly identical for both ridges, as can easily be checked by considering the two representative points of Fig. 7. It consequently appears that the semicircular ridge has all the favorable features of its rectangular counterpart, and shows, in addition, considerable improvement in power handling capacity.

#### Experimental Verification

To obtain an idea of the accuracy of the curves, it was decided to check two points where the accuracy was expected to be low. These points were relative to the  $TE_{01}$  mode (the nets of which contained, in general, fewer points than for the  $TE_{10}$  mode) and to a waveguide with aspect ratio  $b/a=0.466$  (namely the RG-49/U guide). The value of the cutoff wavelength, for insertion coefficients of 0.5 and 0.75, was found, by interpolation from the curves, to be 4.15 cm and 3.95 cm respectively. The measured values were 4.25 cm and 4.08 cm, off by 2 or 3 per cent. This discrepancy is within the limits of the expected 2 per cent over-all accuracy, if one takes into account the additional error introduced by the interpolation process.

#### APPENDIX

The following details about the computation method are of interest:

- 1) Each mode has certain symmetry or antisymmetry properties with respect to the  $0x$  and  $0y$  axes (Fig. 1). The  $TE_{10}$  mode, for example, is symmetrical for  $0x$ , and antisymmetrical for  $0y$ . These properties allow computations to be restricted to a quarter of the cross section.
- 2) The boundary condition  $\phi=0$  is imposed by setting  $\phi_{1''}=\phi_{2''}=0$  in (5). The condition  $\partial\phi/\partial n=0$  is imposed by the use of Fox's method,<sup>6</sup> which consists of computing the value at  $c'$  (see Fig. 2) with the formula

<sup>6</sup> L. Fox, "Solution by relaxation methods of plane potential problems with mixed boundary conditions," *Quart. Appl. Math.*, vol. 2, pp. 251-257; October, 1944.

relative to an ordinary point, *i.e.*, (4). The values of the function at  $2'$  and  $1'$  are taken to be the same as in  $2'''$  and  $1'''$ , points situated on the perpendicular to the boundary, and where  $\phi$  can be obtained by interpolation between  $\phi_e$ , and  $\phi_3$ ,  $\phi_e$ , and  $\phi_4$ , respectively.

3) Iteration with formulas (4) and (5) increases the proportion of lowest modes in the initial distribution  $\phi^0$ . Indeed, the iteration process consists essentially of solving  $\nabla^2\phi^1=-(k^0)^2\phi^0$ . Assuming the initial distribution to be expanded in the still unknown eigenfunctions  $\phi_1$ ,  $\phi_2$ ,  $\dots$ ,  $\phi_n$ ,  $\dots$ , as

$$\phi^0 = c_1\phi_1 + c_2\phi_2 + \dots + c_n\phi_n + \dots \quad (6)$$

Then the "better" approximation  $\phi^1$  is seen to be

$$\phi^1 = c_1 \frac{(k^0)^2}{(k_1)^2} \phi_1 + \dots + c_n \frac{(k^0)^2}{(k_n)^2} \phi_n + \dots \quad (7)$$

and, because  $k_1^2 < k_2^2 < k_3^2, \dots$ , the coefficient of the lowest mode  $\phi_1$  has been proportionally increased as compared to the coefficients of  $\phi_2$ ,  $\phi_3$ ,  $\dots$ , (and similarly for the coefficient of  $\phi_n$  as compared with  $\phi_{n+1}$ ,  $\phi_{n+2}$ ,  $\phi_{n+3}$ , etc.). Convergence will then be ultimately to the lowest mode  $\phi_1$ , whatever the initial distribution  $\phi^0$ , except if  $c_1=0$ , *i.e.*, the initial distribution was orthogonal to  $\phi_1$ . This was fortunately easy enough to ensure in the present problem. Assume that one tries to converge to the  $TE_{10}$  mode, the eigenfunction of which is  $\phi_2$ . The lowest eigenfunction  $\phi_1$  is a constant, *i.e.*, independent of position. If one takes the initial distribution to be symmetrical for  $0x$ , antisymmetrical for  $0y$  (as  $\phi_2$  should be), then  $c_1$  is automatically zero, and convergence will be to the desired eigenfunction  $\phi_2$ . Similarly, symmetry properties allow convergence for the  $TE_{01}$  mode without any trouble. The  $TE_{20}$  mode, however, must be treated carefully. It is symmetrical with respect to  $0x$  and  $0y$ , so that  $c_1$  is not automatically zero anymore; coefficient  $c_1$  is kept equal to zero only if, after each iteration, the function  $\phi$  is adjusted, by addition of a constant, to have an average value equal to zero.

